PNAS

Supporting Information for

Combined disruption of T cell inflammatory regulators Regnase-1 and Roquin-1 enhances anti-tumor activity of engineered human T cells

David Mai[a,b], Omar Johnson[b], Jordan Reff[b], Ting-Jia Fan[b], John Scholler[b], Neil C. Sheppard[b,c,*], Carl H. June[b,c,*]

*Correspondence: Neil C. Sheppard or Carl H. June

Email: neil.sheppard@pennmedicine.upenn.edu, cjune@upenn.edu

This PDF file includes:

Figures S1 to S18
Tables S1 to S2

Other supporting materials for this manuscript include the following:

N/A

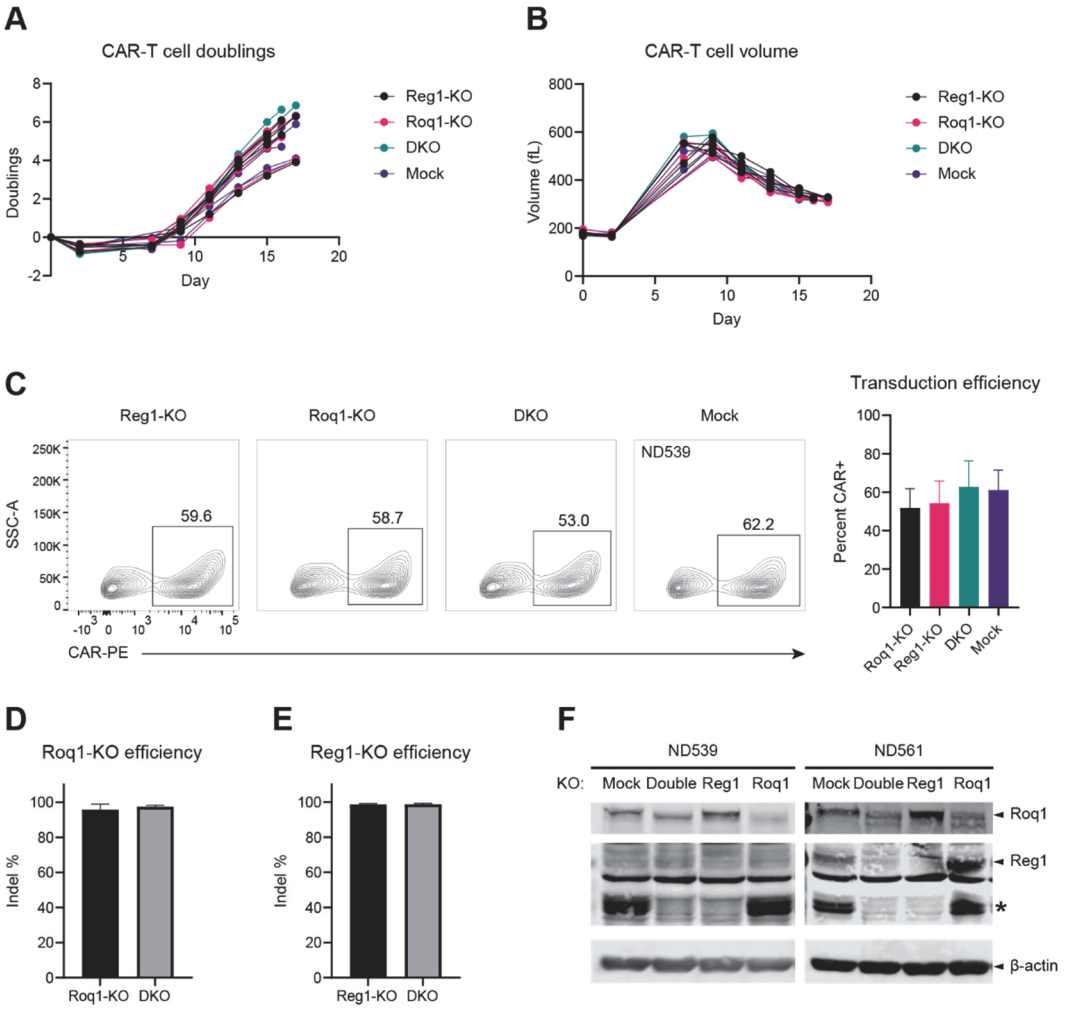

Fig. S1. Expansion and characterization of Regnase-1 and/or Roquin-1 knockout mesothelin-targeting M5 CAR-T cells. (A) Population doublings and (B) cell volumes over time of CAR-T cells during primary expansion. Each line represents an individual donor of an experimental group. (C) Transduction efficiencies of Regnase-1 and/or Roquin-1 knockout CAR-T cells. Flow plots shown are of one representative donor. (D) Roquin-1 and (E) Regnase-1 knockout efficiency of respective Roquin-1 knockout or Regnase-1 knockout, and double knockout cells as measured by percentage of indels at the knockout locus. Indel percentages shown are pooled from all donors. (F). Protein level quantification of Regnase-1 and Roquin-1 in knockout cells by Western blot. Asterisk represents a cleavage product derived from Regnase-1 that more readily appears than the full-length product.

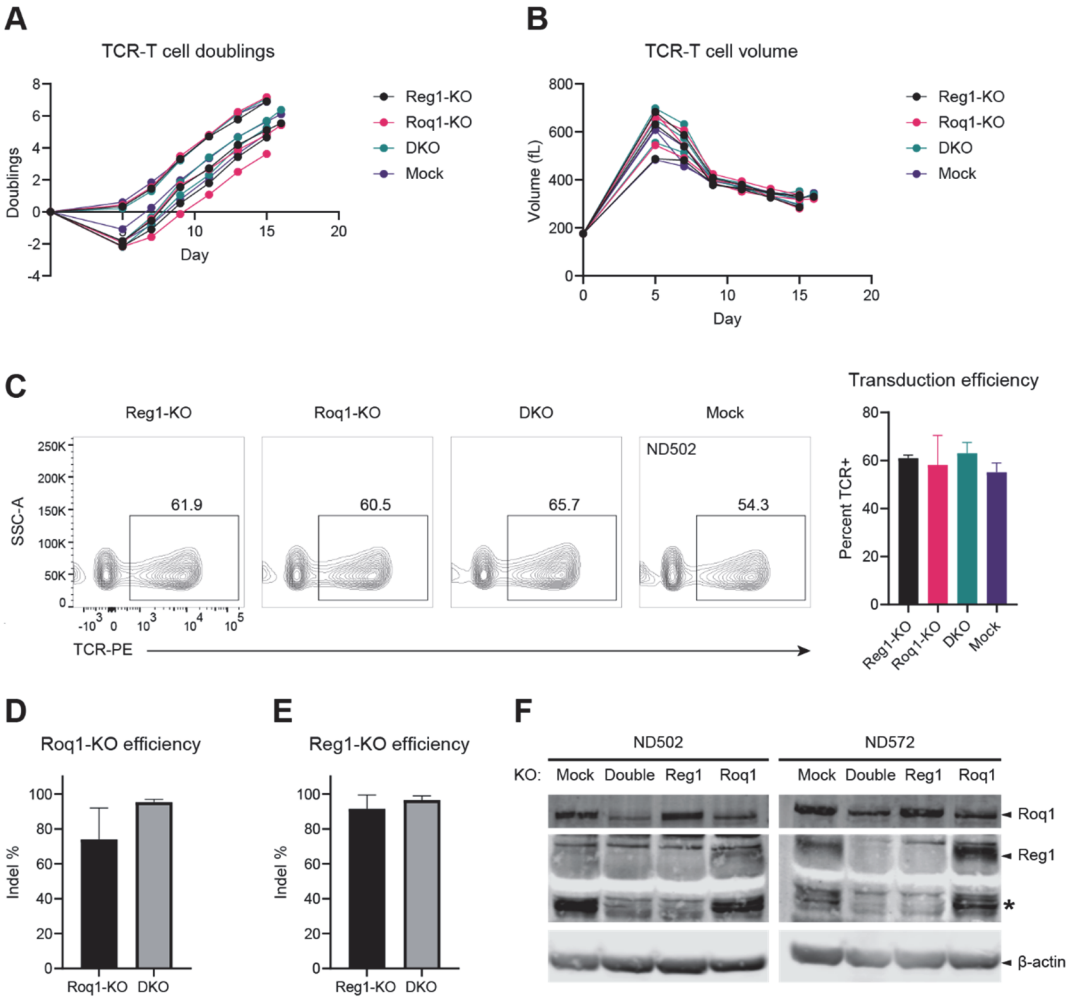

Fig. S2. Expansion and characterization of Regnase-1 and/or Roquin-1 knockout NY-ESO-1-targeting 8F TCR-T cells. (A) Population doublings and (B) cell volumes over time of TCR-T cells during primary expansion. Each line represents an individual donor of an experimental group. (C) Transduction efficiencies of Regnase-1 and/or Roquin-1 knockout TCR-T cells. Flow plots shown are of one representative donor. (D) Roquin-1 and (E) Regnase-1 knockout efficiency of respective Roquin-1 knockout or Regnase-1 knockout, and double knockout cells as measured by percentage of indels at the knockout locus. Indel percentages shown are pooled from all donors. (F). Protein level quantification of Regnase-1 and Roquin-1 in knockout cells by Western blot. Asterisk represents a cleavage product derived from Regnase-1 that more readily appears than the full-length product.

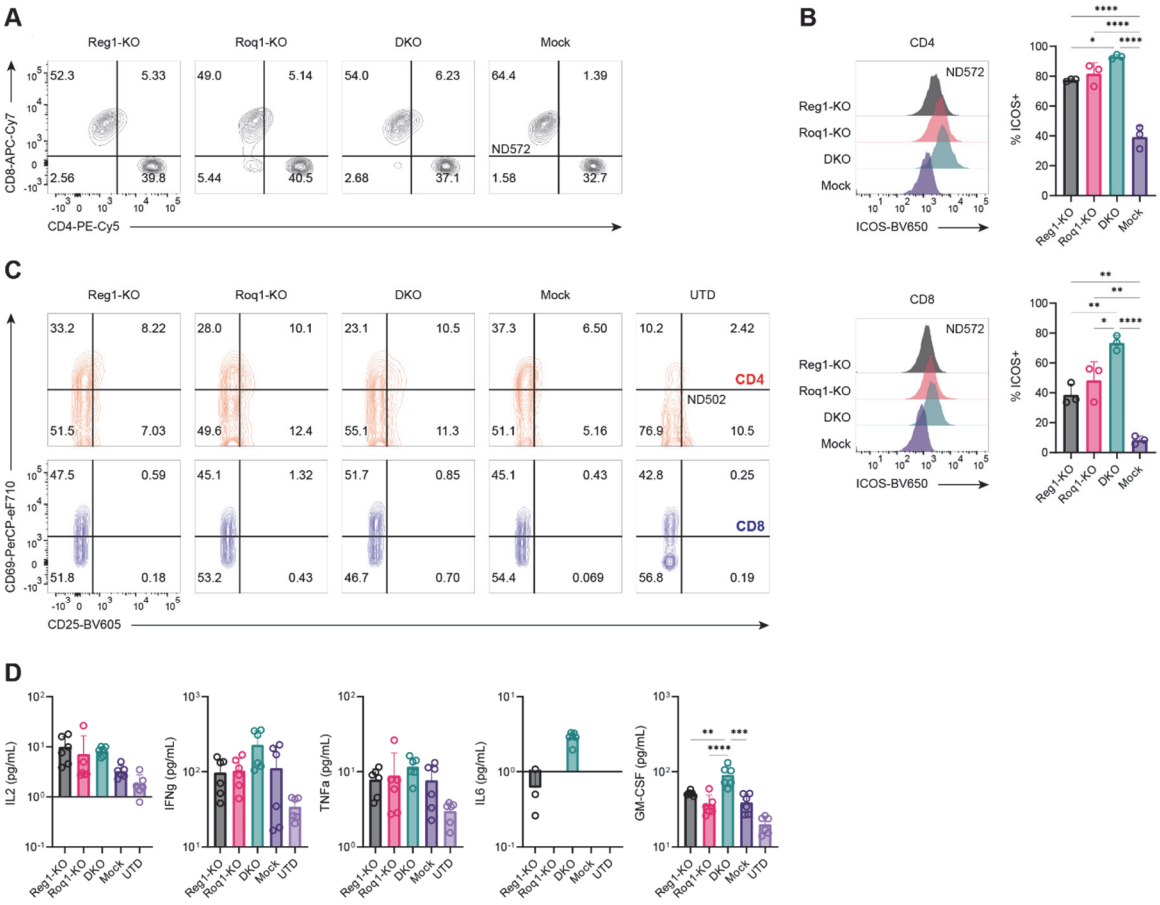

Fig. S3. Baseline profiling of Regnase-1 and/or Roquin-1 knockout TCR-T cells. (A) CD4 and CD8 distribution of TCR-T cells after primary expansion. CD8 knockout cells display slightly enhanced CD4 expression, indicative of a more activated state compared to Mock cells but is not as pronounced as the same observation in CD8 CAR-T cells. Plots shown are representative of 3 independent donors. (B) Expression of ICOS from TCR-T cells rested overnight with cytokines. Left flow plots shown are representative of 3 independent donors. Right graphs show percentage of ICOS+ T cells summarized among 3 independent donors. Error bars represent SD. (C) Expression of activation markers CD25 and CD69 on CD4 (red) or CD8 (blue) TCR-T cells and UTD controls after co-culture with NY-ESO-1-negative Nalm6 cells overnight. Plots shown are representative of 2 independent experiments from 2 independent donors each performed in triplicate. (D) Secretion of Th1 and inflammatory cytokines (IL2, IFNg, TNFa, IL6, GM-CSF) measured via Luminex assay. TCR-T cells and untransduced (UTD) T cell controls were co-cultured with NY-ESO-1-negative Nalm6 cells overnight and supernatants were collected for analysis. Data shown is pooled from 2 independent experiments from 2 independent donors each performed in triplicate. Error bars represent SD. One-way ANOVA was used for analysis followed by Tukey's multiple comparisons test. Not shown = not significant, *P ≤ 0.05; **P ≤ 0.01; ***P ≤ 0.001; ****P ≤ 0.0001.

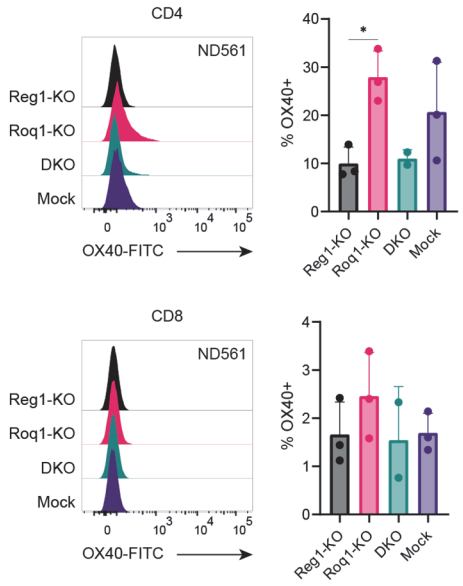

Fig. S4. OX40 expression of baseline CD4 and CD8 T cells. Left flow plots shown are representative of at least 2 independent donors. Right graphs show percentage of OX40+ T cells summarized among at least 2 independent donors. Error bars represent SD. One-way ANOVA was used for analysis followed by Tukey's multiple comparisons test. Not shown = not significant, *P ≤ 0.05; **P ≤ 0.01; ***P ≤ 0.001; ****P ≤ 0.0001.

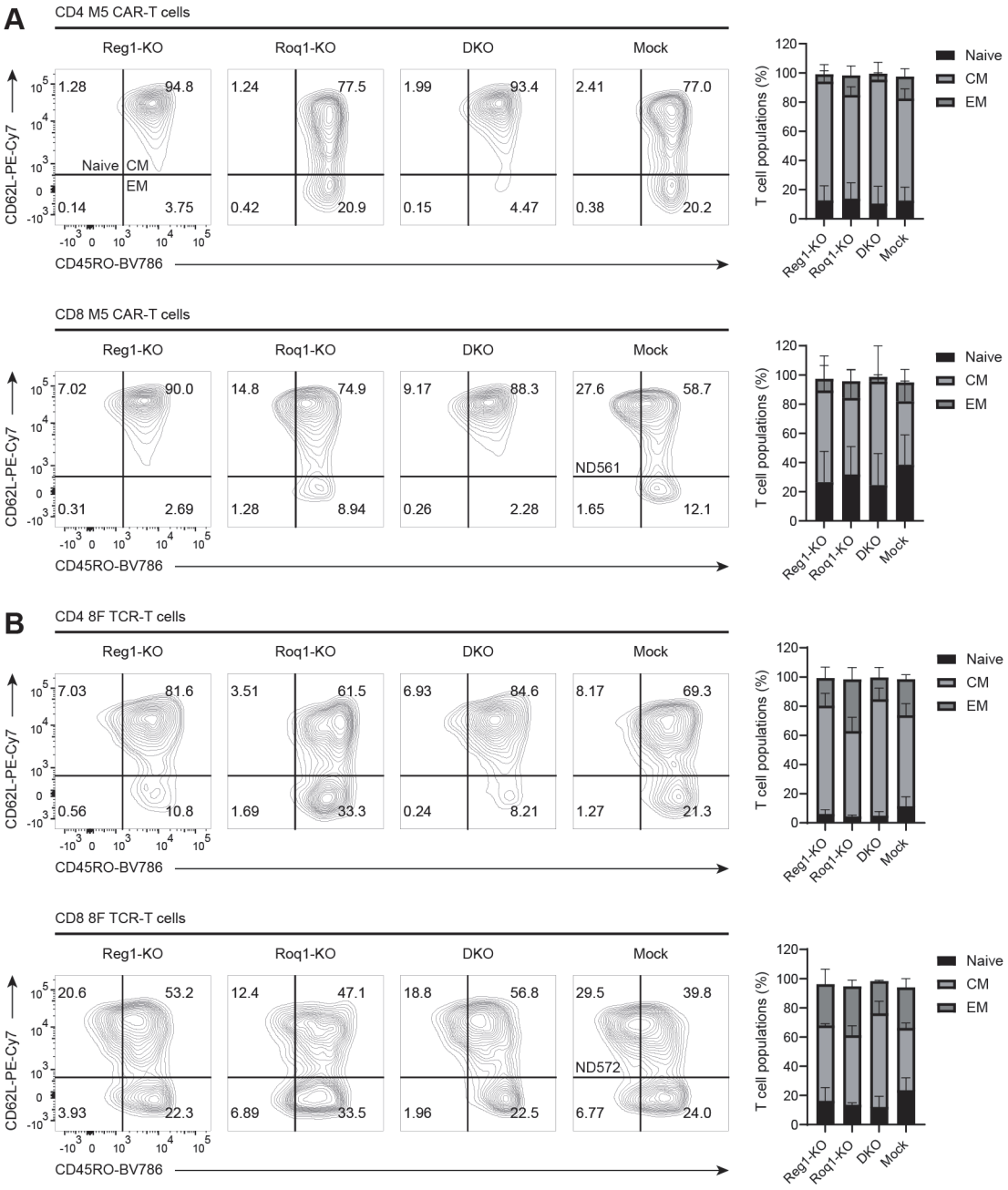

Fig. S5. Baseline T cell subset distributions in Regnase-1 and/or Roquin-1 knockout cells. Regnase-1 knockout and double knockout (A) CAR-T cells and (B) TCR-T cells maintain greater CD45RO+CD62L+ central memory subpopulations compared to Roquin-1 knockout and Mock cells in both CD4 and CD8 cells. Left flow plots are representative of at least 2 independent donors. Right graphs are data pooled from at least 2 independent donors. Error bars represent SD.

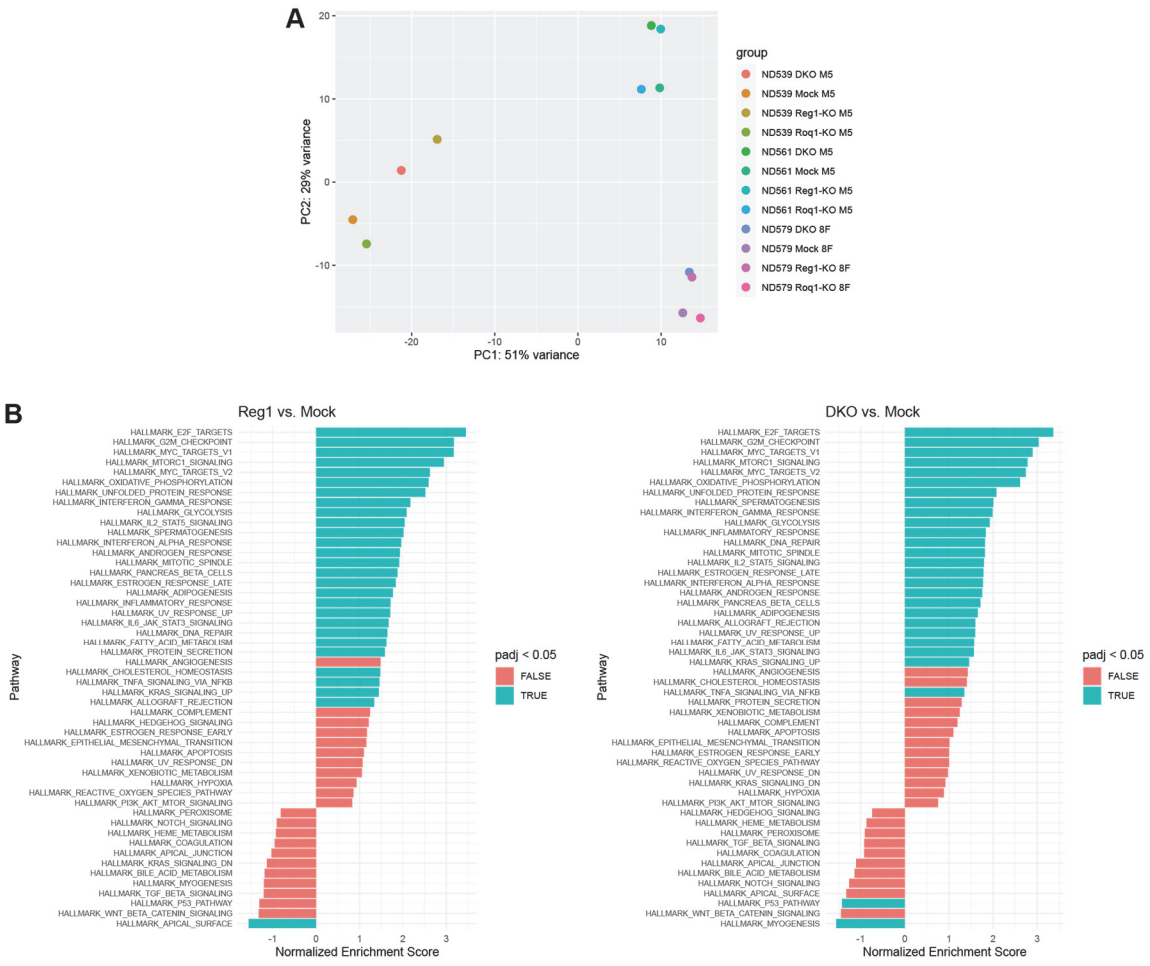

Fig. S6. PCA and pathway analysis of Regnase-1 and/or Roquin-1 knockout engineered T cells. (A) PCA clustering of Regnase-1 and/or Roquin-1 knockout CAR-T or TCR-T cells from 3 independent donors reveals biological differences between donors as the largest source of variance but that within each donor cluster, Regnase-1 knockout and double knockout cells pair more closely and Roquin-1 knockout and Mock cells pair more closely. (B) Pathway analysis of Regnase-1 knockout and double knockout cells compared to Mock cells reveals an enrichment of pathways related to inflammation and cytokine activity.

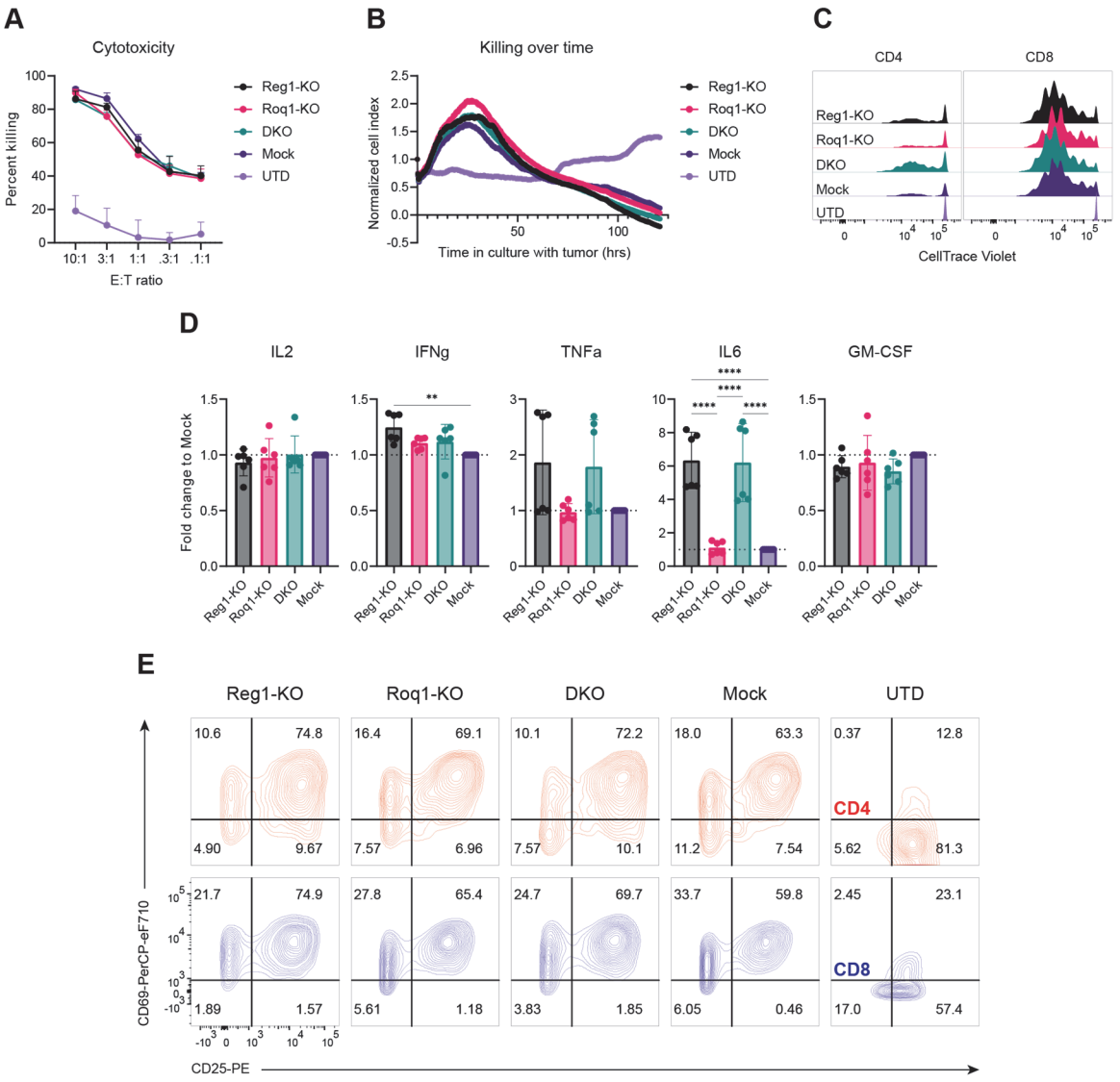

Fig. S7. In vitro functional profiling of Regnase-1 and/or Roquin-1 knockout CAR-T cells. (A) Cytotoxicity of Regnase-1 and/or Roquin-1 knockout CAR-T cells over various E:T ratios. Error bars represent SD. (B) Killing over time of Regnase-1 and/or Roquin-1 knockout CAR-T cells at an E:T ratio of 0.3 with an xCELLigence assay using AsPC1 cells. (C) Proliferation of Regnase-1 and/or Roquin-1 knockout CD4 or CD8 T cells by measuring dilution of CellTraceViolet (CTV) dye. Flow plots shown are representative of 2 independent experiments from 2 independent donors each performed in triplicate. (D) Relative cytokine secretion of knockout cells compared to Mock cells against mesothelin-positive K562 cells. Data shown is pooled from 2 independent experiments from 2 independent donors each performed in triplicate. Error bars represent SD. One-way ANOVA was used for analysis followed by Tukey's multiple comparisons test. (E) Expression of CD25 and CD69 on CD4 (top) or CD8 (bottom) CAR-T cells and UTD controls after co-culture with mesothelin-positive K562 cells overnight. Plots shown are representative of 2 independent experiments from 2 independent donors each performed in triplicate. One-way ANOVA was used for analysis followed by Tukey's multiple comparisons test. Not shown = not significant, *P ≤ 0.05; **P ≤ 0.01; ***P ≤ 0.001; ****P ≤ 0.0001.

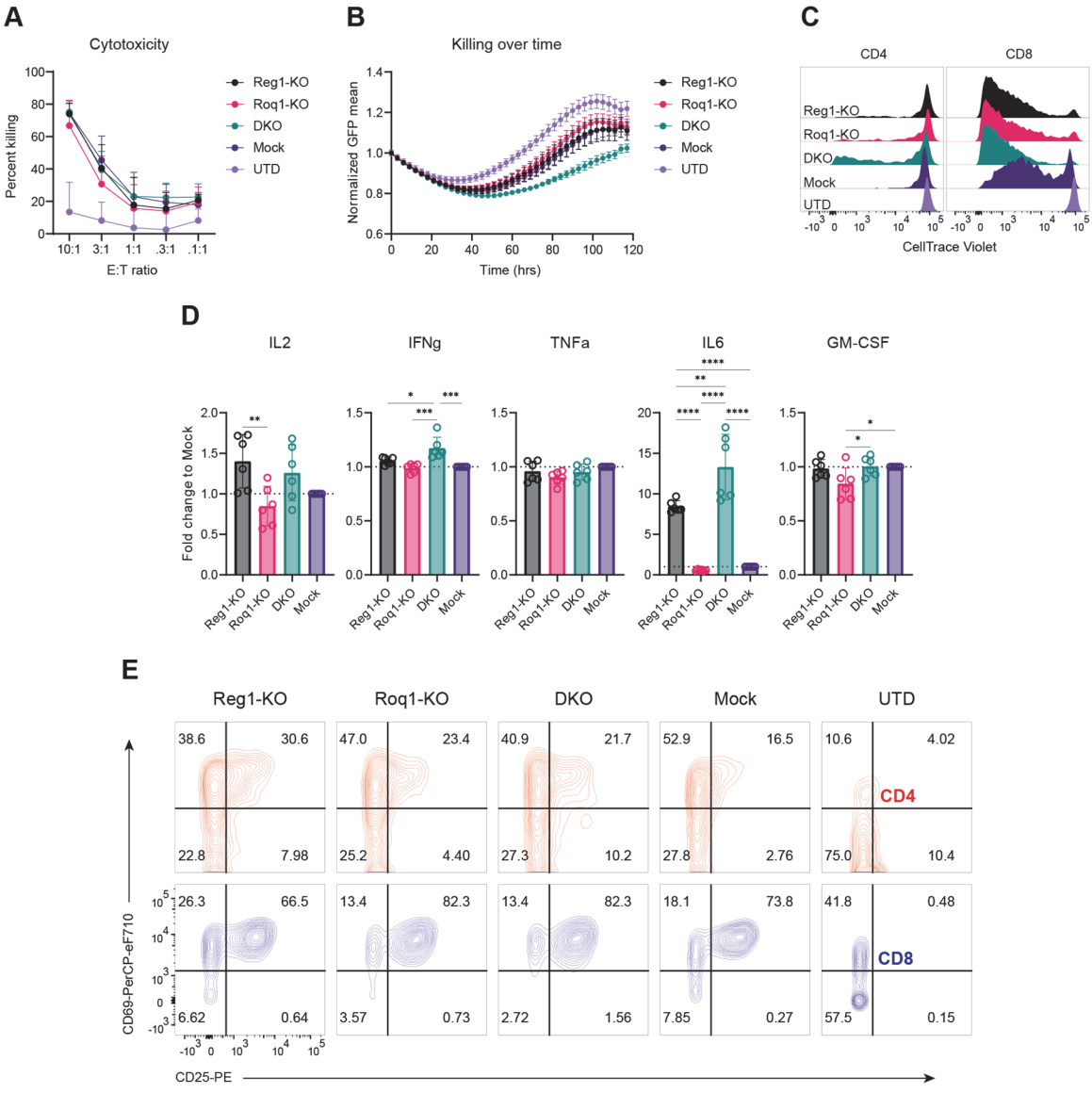

Fig. S8. In vitro functional profiling of Regnase-1 and/or Roquin-1 knockout TCR-T cells. (A) Cytotoxicity of Regnase-1 and/or Roquin-1 knockout TCR-T cells over various E:T ratios. Error bars represent SD. (B) Killing over time of Regnase-1 and/or Roquin-1 knockout TCR-T cells at an E:T ratio of 0.3 with an Incucyte assay using A549-ESO-HLA-II cells. Error bars represent SD. (C) Proliferation of Regnase-1 and/or Roquin-1 knockout CD4 or CD8 T cells by measuring dilution of CellTraceViolet (CTV) dye. Flow plots shown are representative of 2 independent experiments from 2 independent donors each performed in triplicate. (D) Relative cytokine secretion of knockout cells compared to Mock cells against NY-ESO-1-positive Nalm6 cells. Data shown is pooled from 2 independent experiments from 2 independent donors each performed in triplicate. Error bars represent SD. (E) Expression of CD25 and CD69 on CD4 or CD8 CAR-T cells and UTD controls after co-culture with NY-ESO-1-positive Nalm6 cells overnight. Plots shown are representative of 2 independent experiments from 2 independent donors each performed in triplicate. One-way ANOVA was used for analysis followed by Tukey's multiple comparisons test. Not shown = not significant, *P ≤ 0.05; **P ≤ 0.01; ***P ≤ 0.001; ****P ≤ 0.0001.

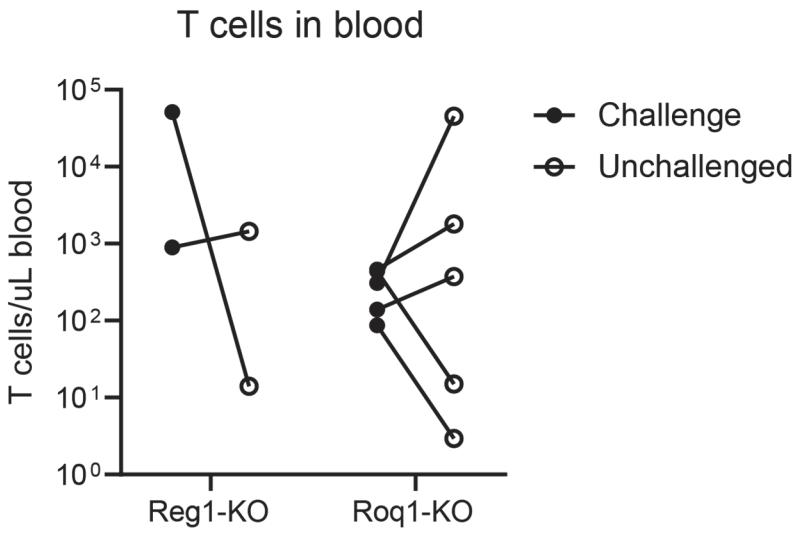

Fig. S9. Changes in peripheral T cell numbers between 21 days after initial tumor challenge (closed circles) and at least one month after initial tumor clearance in mice treated with Regnase-1 or Roquin-1 knockout CAR-T cells (open circles); these mice were not rechallenged with tumor.

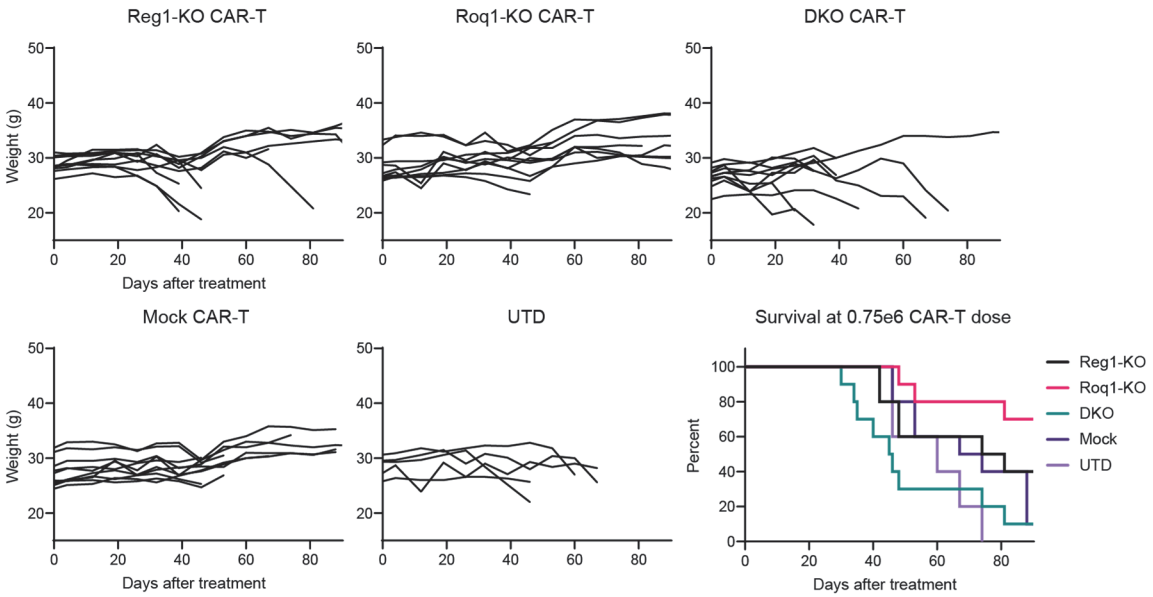

Fig. S10. Weights and survival over time of NSG mice treated at a dose of $0.75x10^6$ CAR-T cells.

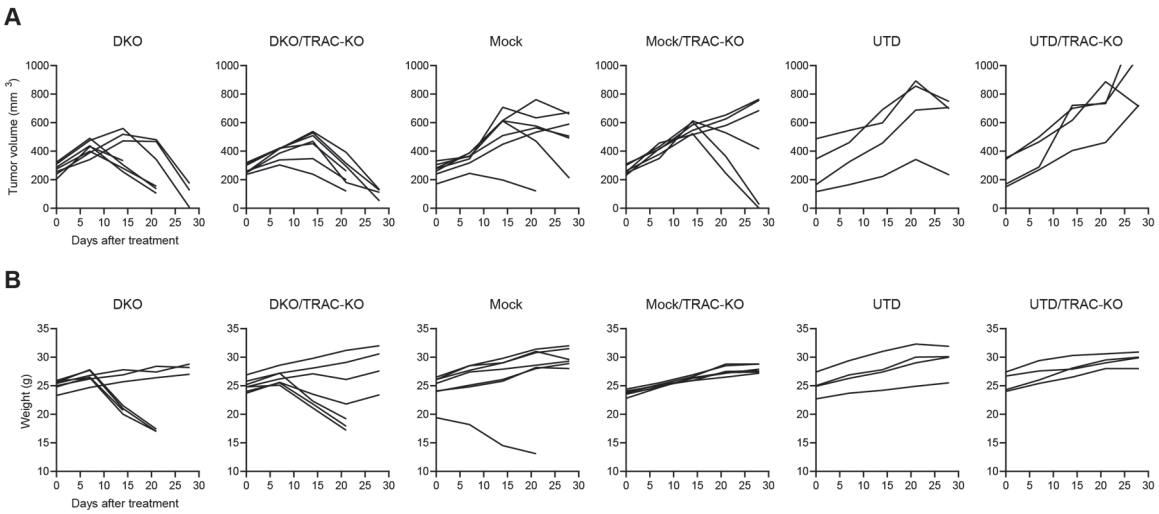

Fig. S11. Tumor control and toxicity of TRAC intact or TRAC-KO Regnase-1 and Roquin-1 double knockout CAR-T cells. (A) Tumor volumes and (B) weights over time of mice treated with $0.5x10^6$ CAR-T cells either with or without TRAC knockout and UTD controls. Data shown is pooled from 2 independent experiments with 2 independent donors.

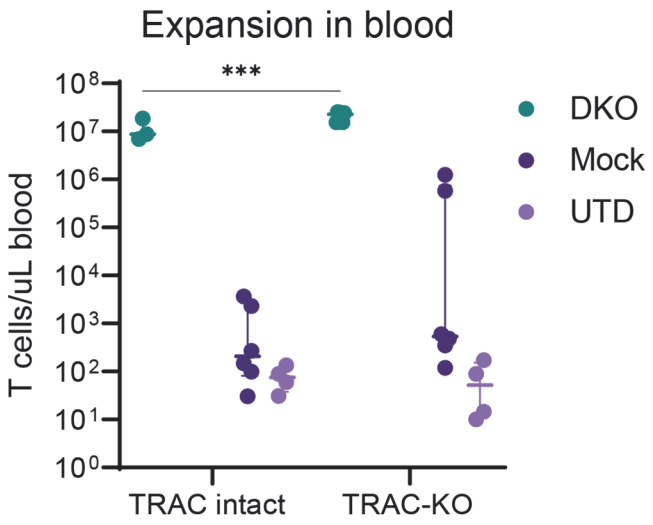

Fig. S12. Expansion of T cells in peripheral blood 21 days after treatment of Regnase-1 and Roquin-1 double knockout CAR-T cells with or without TRAC knockout. Horizontal bars represent median with interquartile ranges. Data shown is pooled from 2 independent experiments with 2 independent donors. Two-way ANOVA was used for statistical analysis followed by Šídák's multiple comparisons test. Not shown = not significant, *P ≤ 0.05; **P ≤ 0.01; ***P ≤ 0.001; ****P ≤ 0.0001.

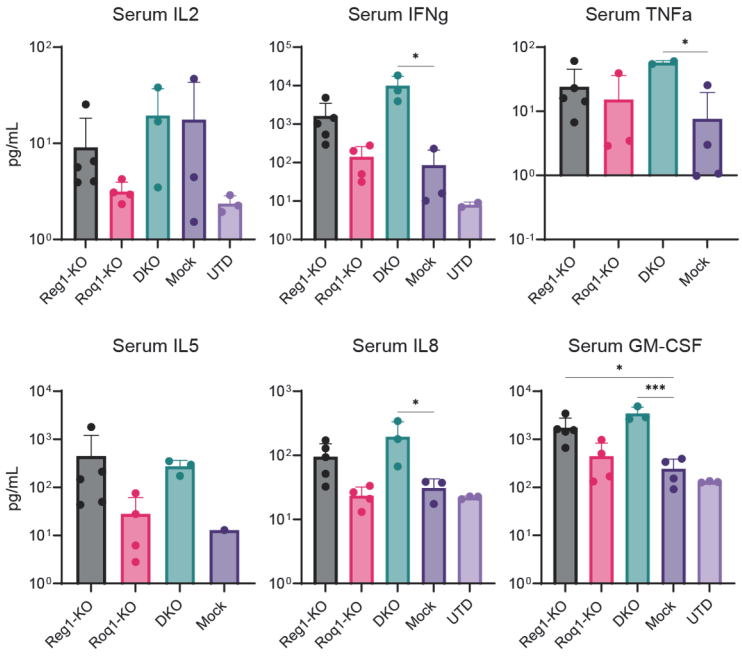

Fig. S13. Levels of human cytokines in mouse serum as measured via Luminex assay from serum samples taken 14 days after CAR-T cell treatment. Error bars represent SD. One-way ANOVA was used for analysis followed by Tukey's multiple comparisons test. Not shown = not significant, *P ≤ 0.05; **P ≤ 0.01; ***P ≤ 0.001; ****P ≤ 0.0001.

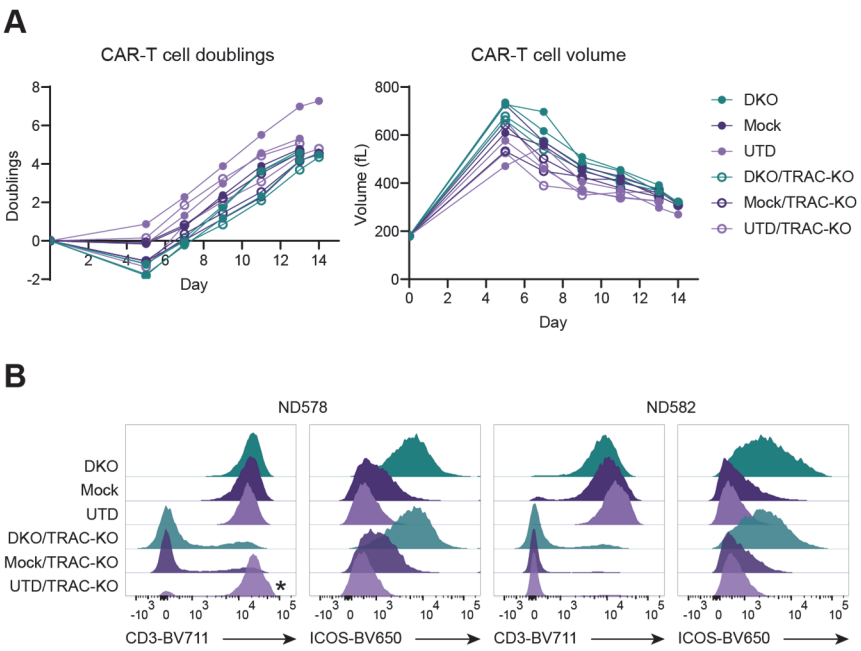

Fig. S14. Expansion and characterization of Regnase-1 and Roquin-1 double knockout CAR-T cells with or without TRAC knockout. (A) Population doublings and cell volumes over time of cells during primary expansion. Each line represents an individual donor of an experimental group. (B) Flow cytometry validation of TRAC knockout as determined by loss of CD3 expression and of Regnase-1 and Roquin-1 double knockout as determined by upregulation of ICOS expression. Asterisk denotes one UTD group in one donor with unsuccessful TRAC knockout that was used in subsequent experiments as TRAC knockout of UTD cells was not expected to alter UTD function as a negative control.

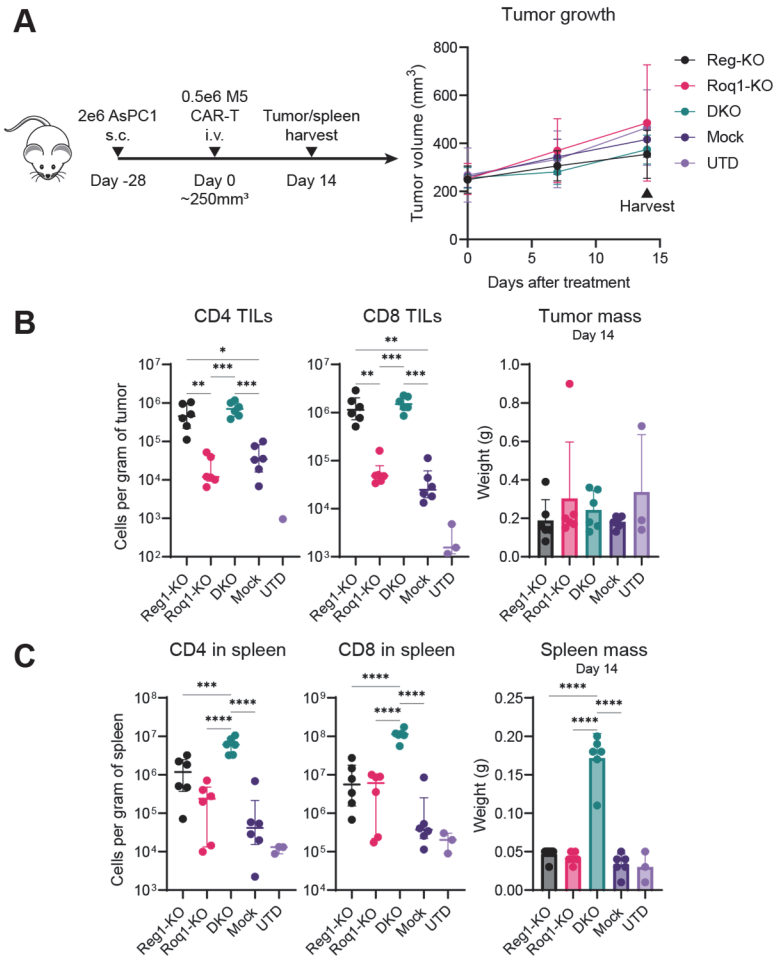

Fig. S15. Enumeration of TILs and T cells in the tumor and spleen from an alternate donor (ND539). (A) Schematic of in vivo mouse experiments to evaluate distribution of T cells and associated tumor growth over time. (B) Quantification of CD4 (left) and CD8 (right) TILs in xenograft tumors and associated weights of individual tumors. (C) Quantification of the number of CD4 (left) and CD8 (right) T cells in mice spleens and associated weights of individual spleens. For cell number quantifications, horizontal bars represent median with interquartile ranges. For quantification of tumor or spleen weights, error bars represent SD. One-way ANOVA followed by Tukey's multiple comparison test was used for statistical analysis. Not shown = not significant, *P ≤ 0.05; **P ≤ 0.01; ***P ≤ 0.001; ****P ≤ 0.0001.

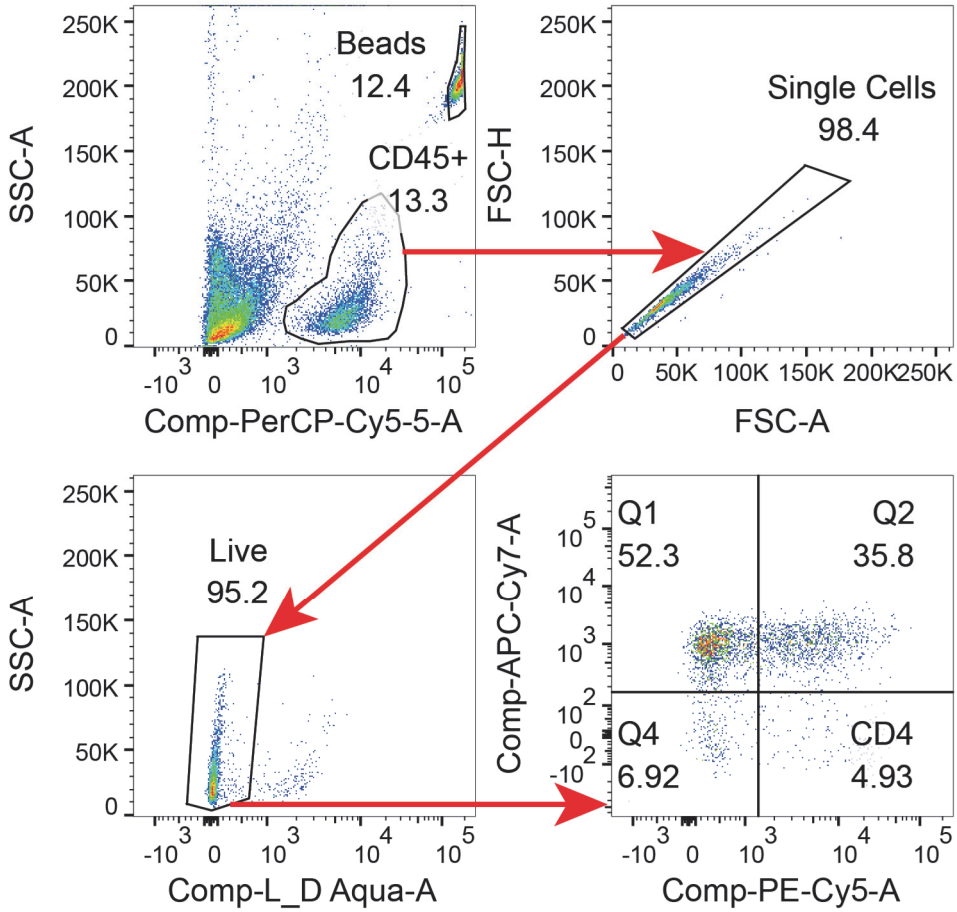

Fig. S16. Example gating scheme for quantifying CD4 and CD8 T cells isolated from mice tumors and spleens.

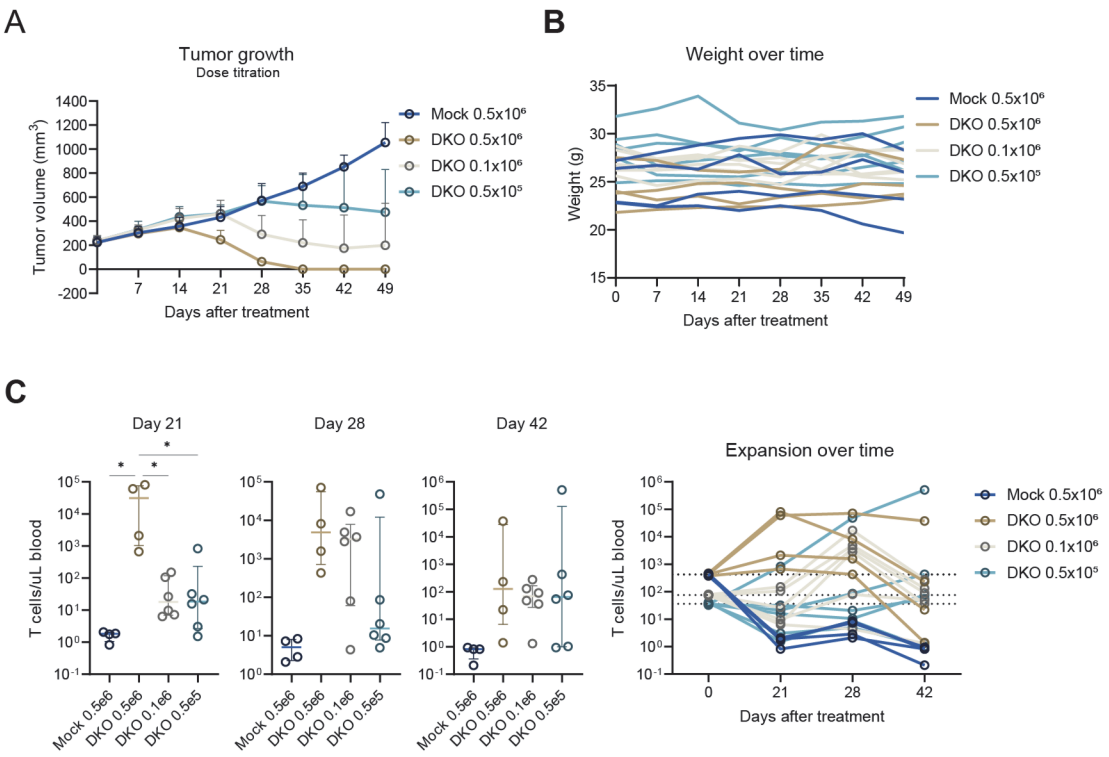

Fig. S17. Evaluating the anti-tumor efficacy of dose titrating DKO mesoCAR-T cells. (A) Tumor volumes and (B) weights over time of NSG mice treated with varying doses of DKO CAR-T cells. Error bars represent SD. (C) Expansion of T cells in peripheral blood 21, 28, and 42 days after treatment of varying doses of Mock or DKO CAR-T cells. Horizontal bars represent median with interquartile ranges. Data shown is pooled from 2 independent experiments with 2 independent donors (n=4 0.5x10^6 Mock, n=4 0.5 x10^6 DKO, n=6 0.1 x10^6 DKO, n=6 0.5 x10^5 DKO). One-way ANOVA was used for analysis followed by Tukey's multiple comparisons test. Not shown = not significant, *P ≤ 0.05; **P ≤ 0.01; ***P ≤ 0.001; ****P ≤ 0.0001.

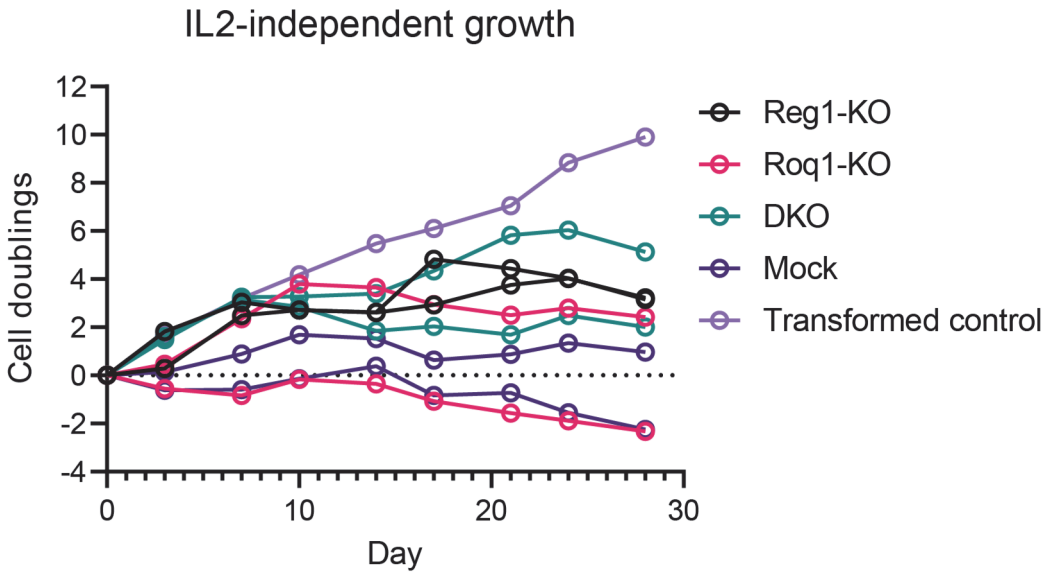

Fig. S18. IL2-independent in vitro growth of KO mesoCAR-T cells. Each line represents an individual donor of an experimental group. Data shown is pooled from 2 independent experiments with 2 independent donors.

Table S1. sgRNA sequences screened for Regnase-1 and Roquin-1 knockout.

Target	sgRNA ID	sgRNA sequence	TIDE KO% (F)	R^2	TIDE KO% (R)	R^2	ICE KO score (F)	R^2	ICE KO score (R)	R^2
ZC3H12A	12A.E2.1	GGACAGGCTTCTCTCCACAG			87.4	0.87	37	0.9	97	0.97
ZC3H12A	12A.E2.2	GGTCATCGATGGGAGCAACG			82.2	0.83	71	0.97	71	0.96
ZC3H12A	12A.E2.3	CGTCCAGGCAGACACCAACA	96.5	0.97	87.2	0.87	79	0.97	78	0.95
ZC3H12A	12A.E2.4	CAGCTCCCTCTAGTCCCGCG	95.4	0.95	93.4	0.93	97	0.97	98	0.98
ZC3H12A	12A.E3.1	CAGTGTTTGTGCCATCCTGG	96.8	0.98			99	0.99	98	0.98
ZC3H12A	12A.E3.2	AAGGAGGTCTTCTCCTGCCG	96.5	0.98	97.6	0.99	99	0.99	99	0.99
RC3H1	H1.E2.1	GCAATGCTGAGTTCACAGGG								
RC3H1	H1.E2.2	TGCCTGTACAAGCTCCACAA								
RC3H1	H1.E2.3	CCTGAATAAACTCCACCGCA								
RC3H1	H1.E2.4	TGGCCACAACCCAAACTGAT								
RC3H1	H1.E3.1	AAGTAATAGGCTGCTGCTCA					78	0.97		
RC3H1	H1.E3.2	TGAAGACACAAAGCATTATG	97	0.97			94	0.98		

Optimal sgRNA sequences chosen for all other experiments are highlighted in yellow.

Table S2. PCR and sequencing primers screened to validate Regnase-1 and Roquin-1 knockout.

Name	Sequence (5' -> 3')	Locus	Direction	Purpose
pcr.12A.E2.F	GTG TGT AGT GCC ACC AAT CC	ZC3H12A Exon 2	Forward	PCR
pcr.12A.E2.R	TTA CCA GTA GCG CGA CCC T	ZC3H12A Exon 2	Reverse	PCR
seq.12A.E2.F	GCG CTA TTC ACC GTC CCT AA	ZC3H12A Exon 2	Forward	Sequencing
seq.12A.E2.R	CCT CCC TCT AGA CCA GTC CC	ZC3H12A Exon 2	Reverse	Sequencing
pcr.12A.E3.F	GGA ACT GGC ACT GGG AAT GGA	ZC3H12A Exon 3	Forward	PCR
pcr.12A.E3.R	AAT GAC CAC CAT TCA GAG CAG G	ZC3H12A Exon 3	Reverse	PCR
seq.12A.E3.F	TCC AAA GGG GAA GGG ACT GC	ZC3H12A Exon 3	Forward	Sequencing
seq.12A.E3.R	TCT CTC TTG GGG AGA ACC AGG	ZC3H12A Exon 3	Reverse	Sequencing
pcr.H1.E2.F	ACT TCC CAT CTC TAA AAT GAG GG	RC3H1 Exon 2	Forward	PCR
pcr.H1.E2.R	AGC GAT CTG CAT AGC TAG GTT	RC3H1 Exon 2	Reverse	PCR
seq.H1.E2.F	GTG GAA TAA GAC TGG ACT TGT GG	RC3H1 Exon 2	Forward	Sequencing
seq.H1.E2.R	AAG CAC TGG ACT ACC ACA ATA A	RC3H1 Exon 2	Reverse	Sequencing
pcr.H1.E3.F	CAA AAC AAA GGA ATG CAA AGA TAC A	RC3H1 Exon 3	Forward	PCR
pcr.H1.E3.R	GTG CAG TAA TGG CAA CTT CCG	RC3H1 Exon 3	Reverse	PCR
seq.H1.E3.F	TGG GCG TTT TGA TGT TAC CAG	RC3H1 Exon 3	Forward	Sequencing
seq.H1.E3.R	TGA TGG AAA GCA CTG CTG AAG	RC3H1 Exon 3	Reverse	Sequencing

PCR and sequencing primers used for all other experiments are highlighted in yellow.